INFECTION AND IMMUNITY, Apr. 2008, p. 1358–1367 Vol. 76, No. 4
0019-9567/08/$08.00+0 doi:10.1128/IAI.01330-07

Bacillus cereus Induces Permeability of an In Vitro Blood-Retina Barrier[▽]

A. L. Moyer,[1] R. T. Ramadan,[2] J. Thurman,[3] A. Burroughs,[4] and M. C. Callegan[1,2,3,5]*

Department of Microbiology and Immunology,[1] Oklahoma Center for Neuroscience,[2] and Department of Ophthalmology,[3] Oklahoma Christian University,[4] and Dean McGee Eye Institute, University of Oklahoma Health Sciences Center,[5] Oklahoma City, Oklahoma

Received 3 October 2007/Returned for modification 6 November 2007/Accepted 28 January 2008

Most *Bacillus cereus* toxin production is controlled by the quorum-sensing-dependent, pleiotropic global regulator *plcR*, which contributes to the organism's virulence in the eye. The purpose of this study was to analyze the effects of *B. cereus* infection and *plcR*-regulated toxins on the barrier function of retinal pigment epithelium (RPE) cells, the primary cells of the blood-retina barrier. Human ARPE-19 cells were apically inoculated with wild-type or quorum-sensing-deficient *B. cereus*, and cytotoxicity was analyzed. *plcR*-regulated toxins were not required for *B. cereus*-induced RPE cytotoxicity, but these toxins did increase the rate of cell death, primarily by necrosis. *B. cereus* infection of polarized RPE cell monolayers resulted in increased barrier permeability, independent of *plcR*-regulated toxins. Loss of both occludin and ZO-1 expression occurred by 8 h postinfection, but alterations in tight junctions appeared to precede cytotoxicity. Of the several proinflammatory cytokines analyzed, only interleukin-6 was produced in response to *B. cereus* infection. These results demonstrate the deleterious effects of *B. cereus* infection on RPE barrier function and suggest that *plcR*-regulated toxins may not contribute significantly to RPE barrier permeability during infection.

Endophthalmitis is inflammation in the eye which often results from the introduction of pathogens into the posterior segment following penetrating eye trauma (posttraumatic), intraocular surgery (postoperative), or metastatic spread to the eye from a distant infection site (endogenous). *Bacillus cereus* causes a uniquely rapid and devastating form of endophthalmitis that can result in loss of vision or of the eye itself in 24 to 48 h (2, 13, 16, 21, 23, 42, 54, 56). *B. cereus* enters the vitreous, where it multiplies and produces toxins, eliciting an explosive inflammatory response (13, 14). This is followed by an influx of polymorphonuclear leukocytes (PMN) into the posterior segment near the retina and optic nerve head as early as 4 h postinfection and by 12 h, greater than 70% of the infiltrated cells in the eye are PMN (49). The breakdown of retinal architecture and loss of vision that follow may be the results of bystander damage to surrounding ocular tissues due to inflammation.

The presence of PMN in the vitreous is atypical because the intraocular environment is designed with anatomical barriers to sequester the tissues from the systemic circulation (58). The outer blood-retina barrier (BRB) is composed of a monolayer of retinal pigment epithelial (RPE) cells that form the outermost layer of the retina. RPE cells, with intercellular tight junctions, form a barrier between the neural retina and the immunologically dynamic choroid.

Ocular inflammation is related to loss of BRB function (22, 68). The breakdown of blood ocular barriers can lead to upregulation of adhesion molecules, leukocyte infiltration (19, 27, 30, 38, 40, 67), and release of inflammatory mediators, which intensify and maintain inflammation (32, 37, 60). BRB permeability occurs during inflammation in an experimental autoimmune uveoretinitis model where leukocytes play an active role in permeability and tight junction disruption (68). However, in *B. cereus* endophthalmitis, the contribution of inflammation and bacterial toxins to BRB function has not been reported.

RPE cells of the BRB may also play a role in inciting the inflammation seen during infection. In vitro studies suggest that RPE cells produce cytokines that contribute to inflammation. Isolated rat RPE cells and human RPE cells have demonstrated antigen-presenting activity (46) and Toll-like receptor (TLR1 to -7, -9, and -10) expression (34), respectively. Inflammatory conditions also stimulated cytokine expression by human RPE cells, including lipopolysaccharide-induced COX-2 (18), interleukin-1α (IL-1α)-induced IL-1β (48), and human cytomegalovirus-induced IL-8 (41). However, the potential role of RPE cells in inflammation during endophthalmitis has not been examined.

During *B. cereus* endophthalmitis, vision loss often occurs despite therapeutic intervention (13, 14). Although antibiotics can sterilize the eye, these drugs are ineffective at preventing intraocular damage from bacterial toxins or the host immune response. Toxin production during the rapid intraocular growth of *B. cereus* contributes to the organism's virulence (21, 23, 42, 56). The production of most *B. cereus* extracellular toxins is regulated globally by the pleiotropic quorum-sensing regulator *plcR* (2, 44). Most of the members of the *B. cereus* group (*B. anthracis*, *B. cereus*, and *B. thuringiensis*) possess *plcR*, though the gene is nonfunctional in *B. anthracis* (2). Individual membrane-damaging toxins under *plcR* regulation, such as phosphatidylcholine-specific phospholipase C (PLC), hemolysin BL, and phosphatidylinositol-specific PLC, contributed minimally to the pathogenesis of experimental *B. cereus* or *B. thuringiensis* endophthalmitis (9, 11). As a group, however, these and other toxins have been shown to be important to the intraocular virulence of *Bacillus* (9, 11). Rabbit eyes infected with *plcR*-deficient mutants of *Bacillus* demonstrated

* Corresponding author. Mailing address: Department of Ophthalmology, DMEI 418, University of Oklahoma Health Sciences Center, 608 Stanton L. Young Blvd., Oklahoma City, OK 73104. Phone: (405) 271-3674. Fax: (405) 271-8781. E-mail: michelle-callegan@ouhsc.edu.
▽ Published ahead of print on 11 February 2008.

significantly greater retinal responses and less inflammation than those infected with wild-type *Bacillus* (15). The *plcR* mutation resulted in a loss of sphingomyelinase, phosphatidylinositol-specific PLC, and phosphatidylcholine-specific PLC activities, as well as a significant decrease in hemolytic and proteolytic activities (52). However, these eyes had significant inflammation and eventually lost retinal function. Therefore, factors not under the control of *plcR* may have contributed to the intraocular virulence observed.

Because significant inflammation occurred during *B. cereus* endophthalmitis, we hypothesized that *Bacillus* infection caused BRB permeability. The extent of inflammation appeared to be related to *plcR* regulation of toxin production. Furthermore, we hypothesized that *Bacillus* growth and toxin production caused RPE cytotoxicity, resulting in tight junction disruption and subsequent barrier permeability. We therefore analyzed whether *B. cereus* infection affects BRB permeability in vitro and whether *plcR*-regulated toxins mediate BRB permeability. Polarized RPE cell monolayers were used to analyze whether *B. cereus* and *plcR*-regulated toxins cause barrier permeability specifically by altering RPE tight junctions. To our knowledge, the effects of infection and inflammation on changes in BRB integrity during endophthalmitis have not been reported. A greater knowledge of the contribution of *plcR*-regulated toxins to barrier dysfunction during a *B. cereus* infection could lead to the identification of potential therapeutic targets that protect the barrier and prevent inflammation and subsequent vision loss in endophthalmitis patients.

MATERIALS AND METHODS

Cell culture and polarization. Human ARPE-19 cells (American Type Culture Collection, Manassas, VA) were propagated in Dulbecco modified Eagle medium (DMEM)/F12 supplemented with 10% fetal bovine serum (FBS) and 1% glutamine (GLN; Gibco, Grand Island, NY). ARPE-19 cells were grown to confluence, diluted in culture medium, and seeded in sterile 24-well plates 48 h before experimentation. Polarized RPE cell monolayers were prepared as follows. Transwells (0.4 μm; Millipore, Billerica, MA) or glass coverslips (Fisher, Waltham, MA) were coated with coating solution (10 ml of DMEM/F12 supplemented with 5% FBS, 1% GLN, 102 μg/ml bovine serum albumin [Fisher], 30 μg/ml bovine type I collagen, and 10 μg/ml human fibronectin [BD Bioscience, San Jose, CA]). After coating, Transwells and coverslips were washed twice with phosphate-buffered saline (PBS) and RPE cells were seeded at 2×10^5/ml in DMEM/F12 supplemented with 5% FBS and 1% GLN. Medium was removed from the apical chamber at 48 to 72 h postseeding to create an air-liquid interface and to stimulate polarization (day 0) (33). Polarized monolayers were incubated for 15 days before infection. Monolayer formation was confirmed by immunocytochemistry, transepithelial resistance (TER) assay, and dextran-fluorophore conjugate transmigration assay. Polarization of monolayers was confirmed by immunoblotting and immunocytochemistry as described below.

Bacterial strains and RPE cell infection. Wild-type *B. cereus* (ATCC strain 14579; BCWT) and the isogenic quorum-sensing *plcR*-deficient *B. cereus* mutant (BC*plcR*::Kan^r) were used in this study (7, 8, 14, 15, 28, 31, 53). Briefly, *plcR*-deficient mutants of *B. cereus* were constructed by insertional inactivation of *plcR* with the kanamycin resistance cassette *aphA3*. A *Bacillus subtilis* laboratory strain was prepared under the same conditions described for *B. cereus*. Cultures of wild-type or mutant *B. cereus* were propagated in brain heart infusion (BHI) medium and diluted into RPE cell culture medium to a final concentration of 10^5 CFU/ml. Suspensions were further diluted to the appropriate inocula of 10^4, 10^3, or 10^2 CFU/ml. Each well was inoculated with 1 ml bacterial solution, and samples were harvested for analysis at 2-h intervals for 8 h. These strains have been shown to infect rabbit and mouse eyes, resulting in explosive inflammation similar to that seen in human cases (12, 49).

Bacterial quantitation. Infected medium was harvested and serially diluted in sterile PBS. Serial 10-fold dilutions were plated on BHI agar in triplicate. Numbers of viable CFU per milliliter are reported as the mean $\log_{10}$ number of CFU ± the standard error of the mean (SEM) for ≥10 analyses per time point.

Analysis of *Bacillus*-induced RPE cytotoxicity. (i) Trypan blue exclusion assay. The viability of infected RPE cell cultures was evaluated by trypan blue exclusion. At various times postinfection, cells were harvested with trypsin-EDTA and pelleted by centrifugation. Pellets were resuspended in equal volumes of PBS, stained with 0.04% trypan blue (vol/vol), and quantified by hemacytometer. Each time point represents six tests, which includes four averaged samples of 50 to 350 cells per sample.

(ii) LDH. The loss of membrane integrity of infected RPE cells was detected with the CytoTox-ONE homogeneous membrane integrity assay (Promega, Madison, WI) according to the manufacturer's instructions. Briefly, monolayers were infected with *B. cereus* and cell supernatants were harvested for analysis of lactate dehydrogenase (LDH) release. LDH was quantified by fluorimetry at an excitation wavelength of 560 nm and an emission wavelength of 590 nm. Controls included freeze-thaw-lysed cells (100% lysis) and untreated cells (0% lysis).

(iii) Flow cytometric analysis. Flow cytometry was used to distinguish between necrotic and apoptotic RPE cell death. ARPE-19 cells were seeded into six-well plates at 5×10^4/ml and inoculated with 10^2 CFU/ml *Bacillus*. At various times postinfection, cells were trypsinized, washed in PBS, and resuspended in 200 μl of diluted binding buffer (Beckman Coulter, Fullerton, CA). A 0.1 M concentration of H_2O_2 was added to the medium at a final concentration of 300 μM (apoptotic control) or 1 mM (necrotic control) (5). Annexin V and propidium iodide (PI; Beckman Coulter) were added to the 200-μl suspension to final concentrations of 0.25 and 25 μg/ml, respectively. After incubation in the dark, 800 μl of binding buffer was added to each sample. Apoptotic or necrotic cell death was then evaluated in reference to untreated samples on a Coulter EPICS XL flow cytometer (Beckman Coulter, Miami, FL).

(iv) Immunoblotting, densitometry, and immunocytochemistry. For immunoblot analysis, lysates of adherent and nonadherent RPE cells were prepared by incubation in Cell Lysis Buffer (Cell Signaling, Danvers, MA) prepared with 20 μg/ml leupeptin (Sigma). Lysate samples prepared at 50 μg were analyzed by gel electrophoresis. Proteins were visualized by Coomassie blue staining or transferred to nitrocellulose for immunoblotting. Membranes were blocked with 5% nonfat milk in 0.1% Tween 20 in Tris-buffered saline for 1 h at 25°C or overnight at 4°C. Membranes were treated with primary antibody overnight at 4°C and secondary antibody for 1 h at 25°C. All antibodies were prepared in 0.1% Tween 20 in Tris-buffered saline with 0.02% NaN_3. Membranes were developed with the ECL Plus Detection System (GE Healthcare, Piscataway, NJ) and imaged on a Storm 860 Imager (Amersham Biosciences, Pittsburgh, PA). Densitometry was performed with ImageQuant software. Expression was calculated in arbitrary units and was normalized to glyceraldehyde-3-phosphate dehydrogenase (GAPDH).

For immunocytochemistry, polarized RPE cell monolayers were permeabilized in ice-cold methanol (20 min at −20°C) and blocked in DakoCytomation protein block (Dako, Carpinteria, CA). Cells were treated with primary antibody for 30 min and with secondary antibody, in the dark, for 30 min. Antibodies were prepared in 0.05 M Tris-HCl–1% bovine serum albumin–50 mM NaN_3. Cells were also treated with 100 nM 4′,6′-diamidino-2-phenylindole (DAPI) in the dark for 3 to 5 min. Coverslips were mounted with fluorescent mounting medium (Dako) and viewed by confocal microscopy (FV 500; Olympus, San Jose, CA).

The antibodies used for immunoblotting and immunocytochemistry included mouse anti-human Na^+/K^+-ATPase (C464.6, 1:100 or 1:500; Chemicon-Millipore), mouse anti-human ZO-1 (specific for the α^+ and α^- isoforms, 1:100; Zymed, San Francisco, CA), mouse anti-human occludin (1:200; Zymed), and anti-mouse immunoglobulin G-horseradish peroxidase (1:5,000; Sigma) or anti-mouse Alexa Fluor 488 (1:200; Molecular Probes-Invitrogen).

Analysis of monolayer permeability. (i) TER assay. Polarized RPE cell monolayers on Transwells transferred to 12-well plates and 2 to 3 ml of cell culture medium were added to the basolateral chamber. Cell culture medium or 10^2 CFU/ml *B. cereus* was added to the apical chamber. The TER across polarized RPE cell monolayers grown was measured with a Millicell-ERS (Millipore, Billerica, MA). Values are expressed as the mean resistance (ohms) per square centimeter ± SEM of six or more samples per time point.

(ii) Dextran transmigration assay. Permeability of polarized monolayers was evaluated by analyzing the diffusion of dextran-fluorophore conjugates through polarized RPE cell monolayers grown on Transwells. A 1-mg/ml concentration of each dextran conjugate was incubated with the apical surface. The concentration of dextran-fluorophores that diffused into the basolateral chamber was quantified by fluorescence spectrophotometry and extrapolated from a standard curve of known concentrations. The fluorophores used included fluorescein isothiocyanate–70-kDa dextran, the size of the blood protein albumin, and tetramethyl rhodamine isocyanate–4-kDa dextran conjugates to examine permeability to smaller blood proteins (Sigma). Values are expressed as the mean [fluorescein isothiocyanate-dextran] ± SEM of six or more samples per time point.

TABLE 1. Sequences of primers used for real-time PCR

Gene product	Primer	Sequence	Size (bp)
β-Actin	Forward	5′-CTC TTC CAG CCT TCC TTC CT-3′	101
	Reverse	5′-TAC AGG TCT TTG CGG ATG TC-3′	
IL-6	Forward	5′-AGT GAG GAA CAA GCC AGA GC-3′	100
	Reverse	5′-GGT CAG GGG TGG TTA TTG C-3′	
MIP-1α	Forward	5′-ACA CCT CCC GAC AGA TTC C-3′	100
	Reverse	5′-CGG CCT CTC TTG GTT AGG A-3′	
TNF-α	Forward	5′-CCC AGG GAC CTC TCT CTA ATC-3′	100
	Reverse	5′-GAG GGT TTG CTA CAA CAT GG-3′	
IL-1α	Forward	5′-TGT GAC TGC CCA AGA TGA AG-3′	100
	Reverse	5′-CCA GAA GAA GAG GAG GTT GGT-3′	

Assessment of inflammatory cytokines. RPE cell monolayers were infected with 10^2 CFU/ml *B. cereus*. At specified times postinfection, cytokine and chemokine mRNA expression was determined by real-time reverse transcription (RT)-PCR. Total RNA was isolated from both adherent and nonadherent cells in accordance with the manufacturer's instructions (Ultraspec RNA Isolation System; BIOTECX, Houston, TX). Following DNase treatment, total RNA was reverse transcribed to produce cDNA by using Moloney murine leukemia virus reverse transcriptase (Promega, Madison, WI) and oligo$(dT)_{12\text{-}18}$ primer (Invitrogen, Carlsbad, CA). All primers were designed to span an intron to control for genomic contamination. Primer efficiencies were verified by performing real-time RT-PCR on a standard curve created with cDNA produced from quantitative PCR total reference RNA (Stratagene, La Jolla, CA). All primers were designed with Ensembl and Primer3. The sequences of the primer sets used are shown in Table 1. The $2^{-\Delta\Delta C_T}$ standard curve method was used to evaluate the relative expression level of targets between treated and untreated RPE cells (36). Real-time PCR was performed (Prism 7000 System; ABI, Foster City, CA) according to the manufacturer's instructions. Briefly, the thermal cycling conditions were 50°C for 2 min and 95°C for 10 min, followed by 40 cycles of 95°C for 15 s and 60°C for 1 min. The cycle threshold (C_T) was set for each target gene, where all amplicons were in the exponential phase of amplification. All PCR products were run on a 0.8% agarose in 0.5% TBE gel to verify the single target amplicon and ensure the absence of genomic contamination. Data were analyzed by the relative standard curve method. All target C_T values reported by the ABI Prism 7000 software were normalized to the endogenous control, β-actin (target mean input/endogenous control mean input = target_N). The resulting C_T value was then normalized to the untreated ARPE-19 control ($\text{target}_N/\text{control}_N$ = relative fold difference in target expression). A greater-than-twofold increase in mRNA expression was considered significant.

For cytokine protein quantification, levels of proinflammatory cytokines and chemokines in cell culture supernatants were quantified with commercial enzyme-linked immunosorbent assay (ELISA) kits (Quantikine; R&D Systems, Minneapolis, MN) in accordance with the manufacturer's instructions. The cytokine and chemokine concentrations were interpolated from standard curves. Values are expressed as the mean ± SEM for six or more analyses per time point.

Statistics. If not stated otherwise, results were the arithmetic means ± SEM of all of the samples in the same experimental group. A two-tailed Student *t* test was used to determine the statistical significance of the data. Statistical significance was determined at $P < 0.05$.

RESULTS

***Bacillus* growth in cell culture medium on ARPE-19 cell monolayers.** To evaluate the contribution of *plcR*-regulated toxin production to RPE function, it was necessary to determine if the wild-type (strain 14579) and *plcR*-deficient (BC*plcR*::Kan^r) *B. cereus* strains grew similarly in cell culture medium on RPE cell monolayers. RPE cell monolayer formation was confirmed by DAPI staining and confocal z-stack imaging, as well as immunocytochemistry for intact tight junction proteins (data not shown). At all time points, 10^2-CFU/ml inocula of wild-type *B. cereus* or the *plcR*-deficient mutant grew to similar concentrations ($P \geq 0.09$) (Fig. 1). All of the other inocula tested resulted in concentrations of greater than 1.0×10^7 CFU/ml at 8 h postinfection. The growth of wild-type *Bacillus* and that of the *plcR*-deficient mutant were also similar ($P \geq 0.99$) in BHI and RPE cell culture media. These results are consistent with previously reported studies of similar wild-type and *plcR*-deficient *B. cereus* growth rates in rabbit eyes and BHI medium (15). The growth of *B. subtilis* also reached 2×10^7 CFU/ml by 8 h, similar to the growth of *B. cereus*.

***Bacillus*-induced RPE cytotoxicity.** Infection with *B. cereus* resulted in rounding of cell bodies and loss of adherence. Cell death occurred in a time- and dose-dependent manner, with wild-type *B. cereus* causing cytotoxicity more rapidly than the *plcR*-deficient mutant. One hundred percent of the RPE cells infected with 10^4 or 10^5 CFU/ml wild-type *B. cereus* were nonviable by 4 h, while infection with 10^3 or 10^2 CFU/ml wild-type *B. cereus* killed 100% of the RPE cells by 6 and 8 h, respectively. The loss of *plcR*-regulated toxin production resulted in a slower rate of RPE cell death. However, there was a complete loss of cell viability, regardless of the infecting strain, by 8 h with the 10^2-CFU/ml inoculations or by 6 h with higher inocula (Fig. 2A). Upon infection of RPE cell monolayers with either strain of *B. cereus*, LDH release occurred in a dose-dependent but strain-independent manner. Loss of membrane integrity occurred at a slower rate upon infection with the *plcR*-deficient *B. cereus* strain. However, by 8 h postinfection there was no significant difference in LDH release upon infection with either strain (Fig. 2B). Overall, *B. cereus* infection appeared to result in significant RPE cytotoxicity that was independent of quorum-sensing-dependent *plcR*-regulated toxin production.

To determine if *B. cereus*-induced cell death occurred by necrosis or apoptosis, we analyzed cell populations by flow cytometry. The dot plots demonstrated a shift of cell populations to the right two quadrants with time, indicating increased PI binding. The dot plots are depicted graphically in Fig. 3. There was an overall decrease in the number of viable cells (annexin V^{Lo}, PI^{Lo}) over the course of infection with either strain, with less than 10% viability by 8 h (Fig. 3B, bottom left quadrant), consistent with trypan blue staining (Fig. 2A). Necrotic cells (annexin V^{Lo}, PI^{Hi}) and secondary/late necrotic

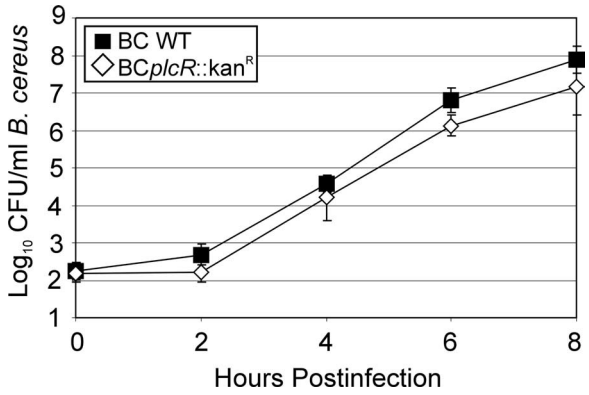

FIG. 1. Growth of *B. cereus* in the presence of ARPE-19 cells. ARPE-19 cell monolayers were infected with 10^2 CFU/ml BCWT (■) or BC*plcR*::Kan^r (◇) at the apical surface. Bacterial concentrations were quantified at 0, 2, 4, 6, and 8 h postinfection, and the two strains grew at similar rates (mean ± standard deviation; six per group).

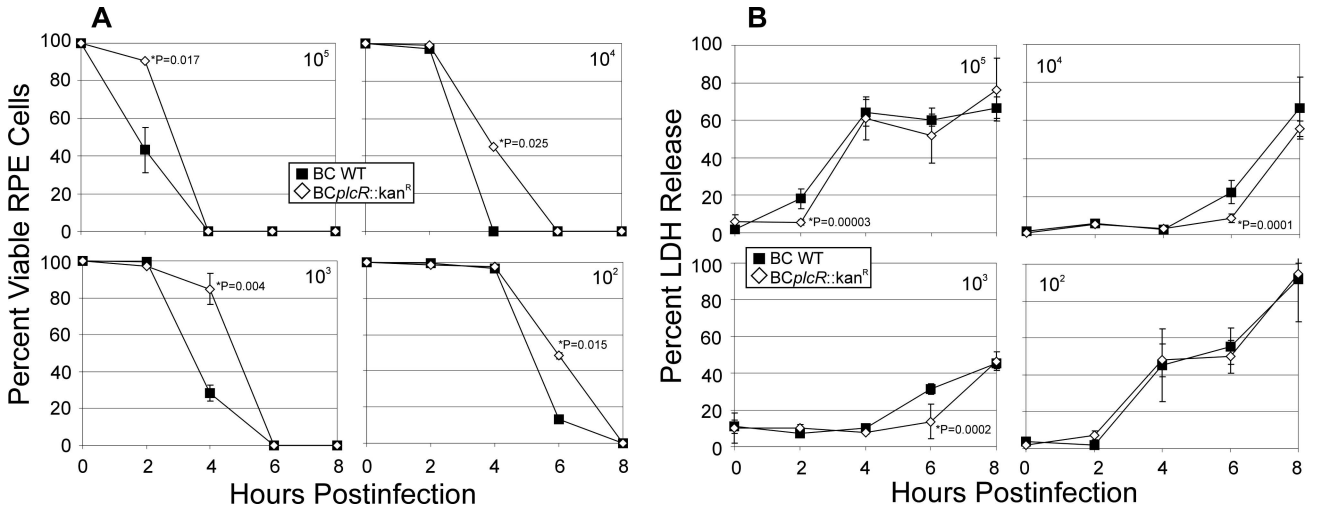

FIG. 2. *B. cereus*-induced RPE cytotoxicity. RPE cell monolayers were infected with 10^2, 10^3, 10^4, or 10^5 CFU/ml wild-type (■) or *plcR*-deficient (◇) *B. cereus*. RPE cells were stained with trypan blue and counted on a hemacytometer (A) (mean ± SEM; six per group). Cytotoxicity occurred regardless of the infecting strain. LDH release also occurred in a dose-dependent manner that was not regulated by *plcR* (B) (mean ± SEM; six per group).

cells (annexin V^{Hi}, PI^{Hi}) both increased with time compared to controls (Fig. 3B, right quadrants). By 8 h postinfection, the total necrotic cell population increased to 86 or 89% after exposure to wild-type or *plcR*-deficient *B. cereus*, respectively. There was a slight increase in the apoptotic cell population (annexin V^{Hi}, PI^{Lo}) from 2% in control cells to 4% in infected cells (Fig. 3B, top left quadrant). These results suggest that infection of RPE cell monolayers with *B. cereus* resulted primarily in *plcR*-regulated toxin-independent necrotic cell death.

Polarized RPE cell monolayers mimic the in vivo BRB. To analyze mechanistic changes in the outer BRB in response to infection, we designed an in vitro system that mimicked the in vivo barrier in structure and function. For RPE cells to have a barrier function in the eye, they must be polarized and have

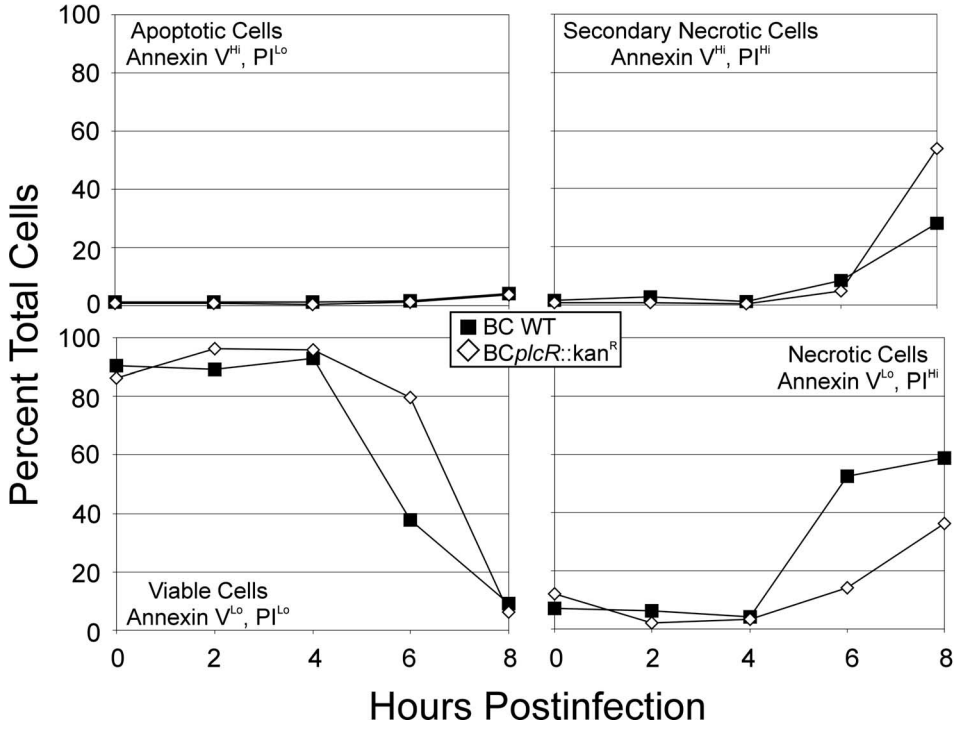

FIG. 3. Necrotic death of RPE cells during infection with *B. cereus*. RPE cell monolayers were infected with 10^2 CFU/ml wild-type (■) or *plcR*-deficient (◇) *B. cereus*. At 0, 2, 4, 6, and 8 h postinfection, cells were harvested and treated with annexin V and PI to identify apoptotic and necrotic cells, respectively. This graphical representation shows that infected cell populations demonstrated a shift from viable to necrotic over time (represents six per group).

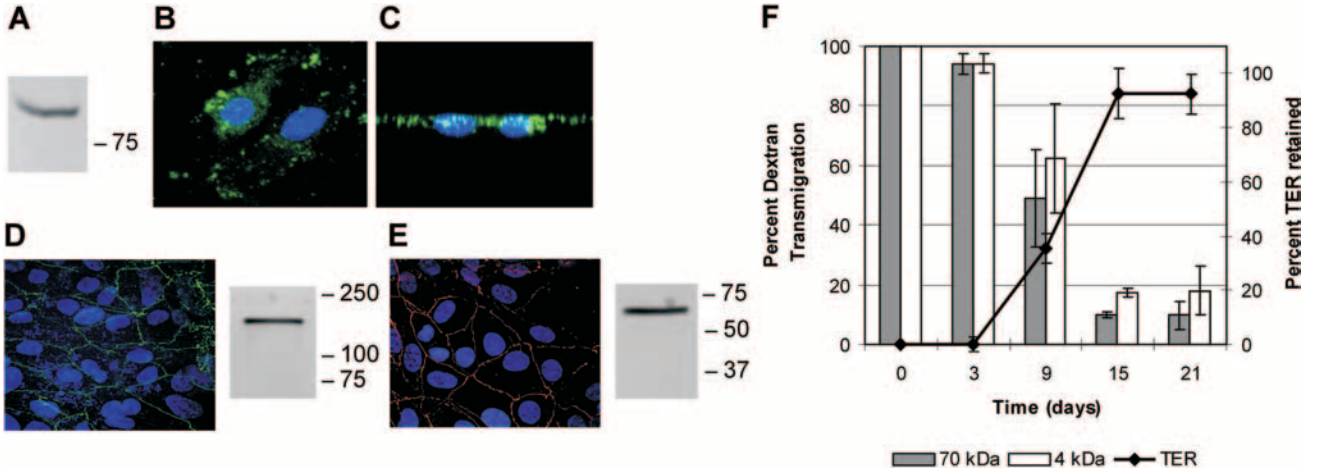

FIG. 4. Polarization of RPE cell monolayers. Abundant expression and apical localization of the RPE Na^+/K^+-ATPase demonstrate polarization. RPE cell monolayers were analyzed by immunoblotting, probing with antibodies to the Na^+/K^+-ATPase (A). RPE cell monolayers were also subjected to immunocytochemistry (B) and are shown as a z-stack confocal image (C). The nuclei (blue) and Na^+/K^+-ATPase (green) were imaged from oblique (B) and z-stack (C) views. ZO-1 (D) and occludin (E) expression and localization were analyzed by immunoblotting and immunocytochemistry. Tight junction proteins localized to the cell membranes. The blots and images are representative of three or more individual blots or experiments. Barrier function was analyzed by dextran transmigration assay and TER assay (mean ± SEM; six per group). TER values (ohms per square centimeter) were normalized to blank Transwell TER values to provide a final calculation of percent TER. Monolayer barrier function was established by day 15 (F). The values to the right of panels A, D, and E are molecular sizes in kilodaltons.

intact, functional tight junctions which are impermeable to blood constituents. We analyzed the expression and localization of the Na^+/K^+-ATPase at the apical surface of polarized RPE cells (6, 24, 43) and found significant apical expression. Cells grew in confluent monolayers with little or no cell overlap, and confocal z-stack imaging illustrated the apical localization of the Na^+/K^+-ATPase (Fig. 4B and C). Polarized RPE cell monolayers also expressed both ZO-1 and occludin at the cell periphery (Fig. 4D and E).

To analyze barrier functionality, TER and dextran-fluorophore transmigration were assessed. TER across the monolayers increased over time and was maintained from 15 (92.47% ± 13.15%) through 21 days (92.33% ± 0.07%) (Fig. 4F). Monolayers exhibited decreased permeability to both 4-kDa and 70-kDa dextran-fluorophore conjugates by 15 days (Fig. 4F). This in vitro model of polarized RPE cell monolayers appeared to be similar, both structurally and functionally, to the in vivo outer BRB.

***B. cereus*-induced RPE cell monolayer permeability.** We next examined the ability of *B. cereus* growth and *plcR*-regulated toxins to perturb the barrier function of polarized RPE cell monolayers. Infection with either strain of *B. cereus* resulted in a rapid decline in TER, indicating permeability of the monolayer. At 4 h, wild-type *B. cereus* induced loss of monolayer TER more rapidly than did the *plcR*-deficient mutant. By 6 h postinfection, 0% of the original TER was retained, regardless of the infecting strain (Fig. 5A). Untreated monolayers retained 100% resistance over the time course. These results suggested that loss of TER, but not the rate of loss, occurred independently of *plcR*-regulated toxins. *B. subtilis*-treated monolayers also retained resistance over time, indicating that the loss of resistance upon infection with *B. cereus* was not merely the result of dense growth of bacteria.

Permeability was also quantified with dextran-fluorophore conjugates. The rate of permeability to the 4-kDa ($P = 0.001$) and 70-kDa ($P = 0.00009$) dextrans was different at 6 h postinfection, with the wild-type *Bacillus* causing permeability more rapidly than the *plcR*-deficient mutant. By 8 h postinfection, there were 17.09-fold and 17.57-fold increases in permeability to 4-kDa dextrans in cells infected with wild-type *B. cereus* and the *plcR*-deficient mutant, respectively ($P < 0.05$) (Fig. 5B). Additionally, the permeability of monolayers to 70-kDa dextrans increased 25.15-fold and 25.02-fold after 8 h of infection with wild-type *B. cereus* and the *plcR*-deficient mutant, respectively (Fig. 5C). Mock-treated monolayers were not permeable to dextran conjugates over the course of infection. Cells treated with 0.1 M H_2O_2 were 21.04-fold more permeable to 4-kDa dextrans and 30.24-fold more permeable to 70-kDa dextrans by 8 h postinfection (Fig. 5C). These data suggested that *B. cereus*-induced permeability of polarized RPE cell monolayers inhibited normal barrier function, regardless of the infecting strain.

Tight junction expression and localization during *B. cereus* infection. Our data indicated that *Bacillus*-induced changes in polarized RPE cell monolayers resulted in barrier permeability. We therefore tested whether permeability was due to changes in intercellular tight junction proteins ZO-1 and occludin. ZO-1 appeared to dissociate from the cell periphery, and its expression decreased from 2 to 6 h postinfection. By 8 h postinfection, no ZO-1 signal was detectable (Fig. 6A). Overall, occludin expression in the polarized RPE cell monolayers was less robust than that of ZO-1, likely due to the heterogeneity that is common in in vitro epithelial cell lines (52). After *B. cereus* infection, the occludin signal was decreased as early as 2 h postinfection. By 4 h postinfection, the occludin signal was almost undetectable by immunocytochemistry (Fig. 6B). By 8 h postinfection, there were no adhered cells visible and occludin and ZO-1 signals were not detectable (data not shown).

Expression of ZO-1 and occludin was also examined by

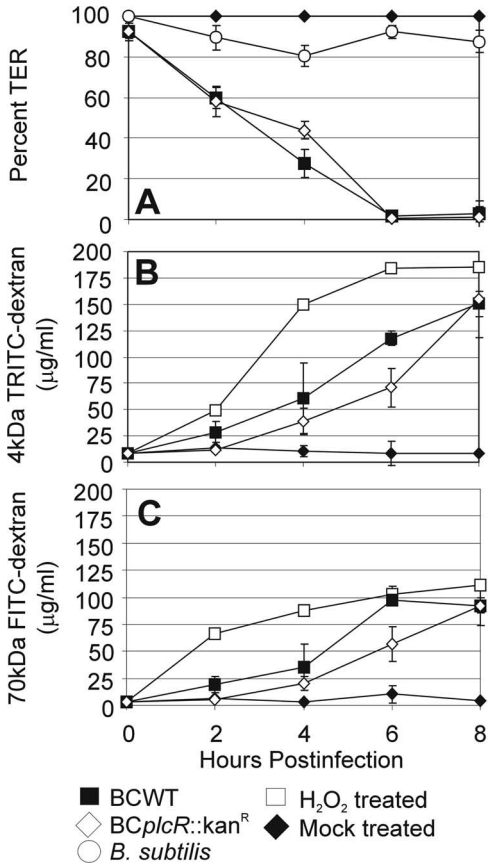

FIG. 5. *B. cereus* infection of polarized RPE cell monolayers results in barrier permeability. Polarized RPE cell monolayers were infected with *B. cereus* (BCWT, ■; BC*plcR*::Kan^r, ◇) or *B. subtilis* (○) at 10^2 CFU/ml at the apical surface, and permeability was analyzed by TER measurement (A) (mean ± SEM; six per group) and dextran transmigration assay (B and C) (mean ± SEM; six per group). In the latter, 4-kDa (B) and 70-kDa (C) dextran-fluorophore conjugates were added to the apical chamber and recovered from the basolateral chamber at the indicated time points. Loss of TER and increased permeability to dextran conjugates indicated permeability of the RPE cell monolayer during *B. cereus* infection.

immunoblotting. ZO-1 expression was decreased at 6 h postinfection, with no detectable expression by 8 h postinfection (Fig. 7A). Similarly, by 6 h postinfection there was no detectable occludin expression (Fig. 7B), consistent with the tight junction perturbation seen in Fig. 6. Changes in the tight junctions of RPE cells may have been a result of *B. cereus* specifically targeting the tight junctions or an indirect result of cytotoxicity. To differentiate between these two possibilities, subsequent immunoblots were analyzed by densitometry to quantify the changes in tight junction proteins. First, the cytotoxicity in polarized RPE cell monolayers was measured and complete cell death occurred by 8 h (Fig. 8A). In Fig. 8B, ZO-1 and occludin expression was measured in viable cells only by normalizing protein expression to GAPDH expression, which is only found in live cells. This excluded the loss of tight junction protein expression seen as a result of cell death. Though Fig. 8A demonstrated a loss of cell viability, there was a decrease in occludin and ZO-1 expression in viable cells prior to death. This suggested that changes in ZO-1 and occludin did not occur merely as a result of cytotoxicity (Fig. 8B).

Proinflammatory cytokine expression during *Bacillus* infection. Because RPE cells have previously been shown to demonstrate immunological activity, we analyzed whether RPE cells could play a role in actively recruiting PMN into the vitreous during infection. To determine if the RPE cells produced proinflammatory cytokines, we evaluated cytokine and chemokine production by real-time RT-PCR and ELISA (Fig. 9). By 6 h postinfection, RPE cells infected with wild-type *Bacillus* exhibited an increase in the transcription of IL-6 mRNA (9.01-fold) and IL-1α mRNA (7.84-fold) (Fig. 9A). Both IL-1α and IL-6 mRNA levels decreased at 8 h postinfection (less than twofold), correlating with cell death by 8 h postinfection (Fig. 2D). However, there was no significant increase in IL-6 or IL-1α mRNA expression from cells infected with the *plcR*-deficient *Bacillus* mutant. There was no expression of MIP-1α or tumor necrosis factor alpha (TNF-α) mRNA during infection with either *B. cereus* strain. ELISA analysis demonstrated that RPE cells infected with wild-type *Bacillus* produced 23.63 ± 2.85 pg/ml IL-6 protein by 8 h postinfection, confirming the real-time PCR results (Fig. 9B). However, no IL-6 was produced by RPE cells infected with the *plcR*-deficient mutant. There was no expression of proinflammatory cytokine protein MIP-1α, TNF-α, IL-1α, IL-1β, or IL-8 during infection with either *Bacillus* strain. Taken together, these results show that RPE cells can produce IL-6 but may not produce most of the proinflammatory cytokines produced during *B. cereus* endophthalmitis.

DISCUSSION

Inflammation during experimental *B. cereus* endophthalmitis may be detrimental to visual function. Normally, the eye is an immunologically privileged environment as a result of a multitude of factors, including the avascular nature of the aqueous humor and vitreous, the presence of blood ocular barriers, the lack of lymphatic drainage pathways (except the uveoscleral drainage pathway), the deficiency of antigen-presenting cells, and immunosuppressive substances in the aqueous humor (20, 29, 58, 60–63). This allows the eye to preserve the clarity of the visual axis. RPE cells are the primary barrier cells of the outer BRB and have a paradoxical function in both managing the blood supply from the fenestrated capillaries of the choroid to the photoreceptors and protecting the neural retina from infiltration of blood constituents. RPE cells contain intercellular tight junctions which form a diffusion barrier. To sustain the relative impermeability of the barrier, tight junction proteins and cytoskeletal proteins must associate at the lateral surface of each cell. ZO-1 and occludin are two tight junction proteins that are structurally and functionally essential for BRB formation and maintenance.

Breakdown of this barrier is associated with almost every retinal disease (17, 37), and infection has specifically been identified as a cause of barrier disruption (18, 45). In human cases of endophthalmitis, significant localization of serum albumin in the BRB has been reported (64). However, neither the extent of barrier breakdown nor its contribution to vision loss during endophthalmitis has been examined in great detail. Therefore, we hypothesized that the invasive and aggressive

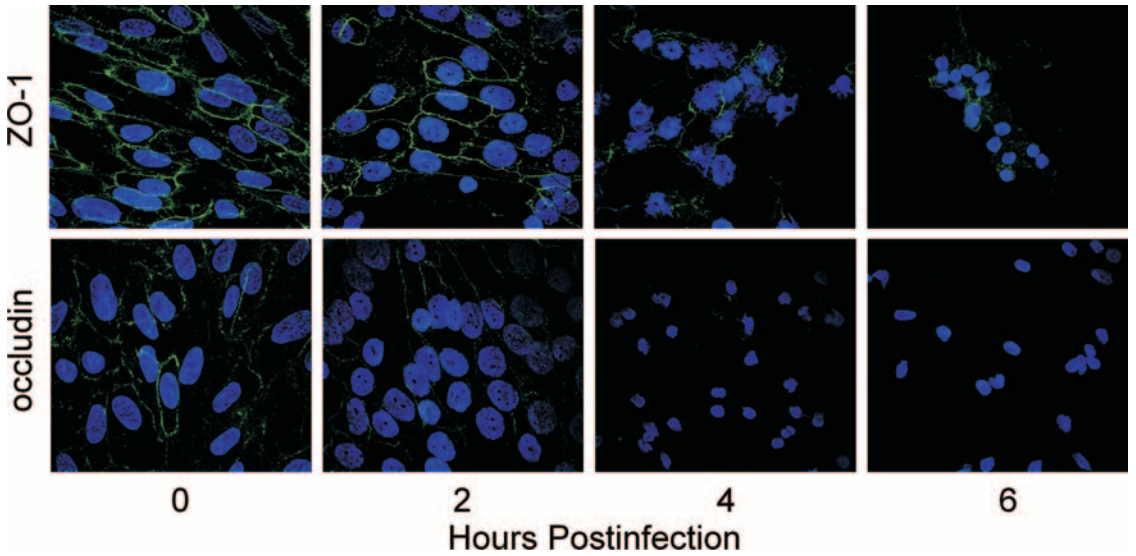

FIG. 6. Changes in ZO-1 and occludin distribution in RPE cell monolayers in response to *B. cereus* infection. RPE cell monolayers were infected with 10^2 CFU/ml *B. cereus* and analyzed by immunocytochemistry for ZO-1 or occludin. Slides were examined by confocal microscopy at ×100 magnification. ZO-1 redistribution away from the cell periphery began at 6 h, and expression was lost by 8 h postinfection. Occludin disruption began as early as 2 h postinfection, and expression was lost by 6 h postinfection. The images are representative of six or more individual experiments.

nature of *B. cereus* and its toxins may damage and compromise the BRB during infection, allowing PMN into the posterior segment. In this study, we investigated the effects of *B. cereus* growth and toxin production on RPE cell viability and analyzed the changes in BRB permeability, tight junction structure and function, and inflammatory cytokine production during *Bacillus* infection.

In this study, RPE cell viability was significantly reduced

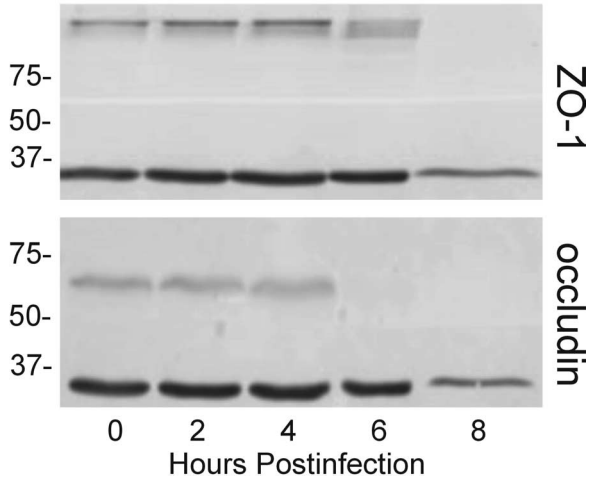

FIG. 7. Changes in ZO-1 and occludin expression in RPE cell monolayers in response to *B. cereus* infection. Polarized RPE cell monolayers were infected with *B. cereus* at 10^2 CFU/ml at the apical surface, and lysates were harvested for analysis by immunoblotting. Membranes were probed with antibodies to ZO-1 (A) and occludin (B). Expression of occludin was lost at 6 h postinfection, while ZO-1 expression decreased but was not lost until 8 h postinfection. The blots shown are representative of three or more individual blots. The values on the left are molecular sizes in kilodaltons.

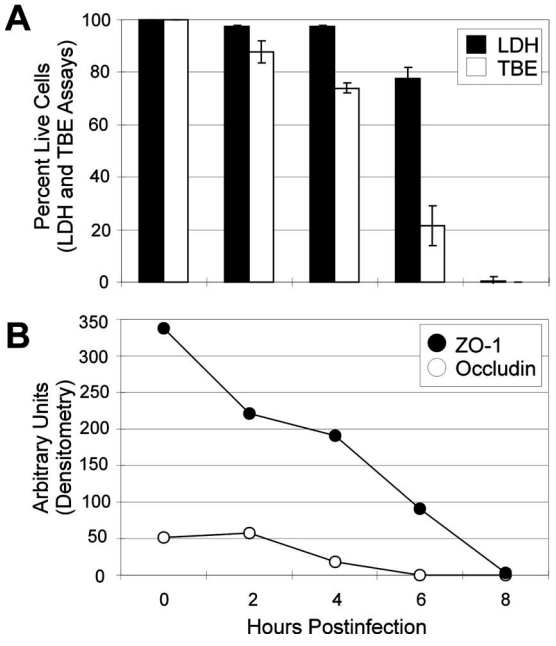

FIG. 8. Loss of ZO-1 and occludin expression in polarized RPE cell monolayers occurs prior to cytotoxicity. Polarized RPE cell monolayers were infected with 10^2 CFU/ml wild-type *B. cereus* and harvested for analysis of cytotoxicity by LDH release assay (black box) and trypan blue exclusion assay (white box) (A). After infection, cell monolayers were also harvested for analysis by immunoblotting. Membranes were probed with antibodies for ZO-1 (●) and occludin (○). Densitometry measurements are expressed in arbitrary units and normalized to GAPDH expression (mean ± SEM; six per group) (B). Units represent the expression of tight junction proteins in viable cells only. Decreased tight junction protein expression occurred in viable cells and correlated with an overall loss of cell viability.

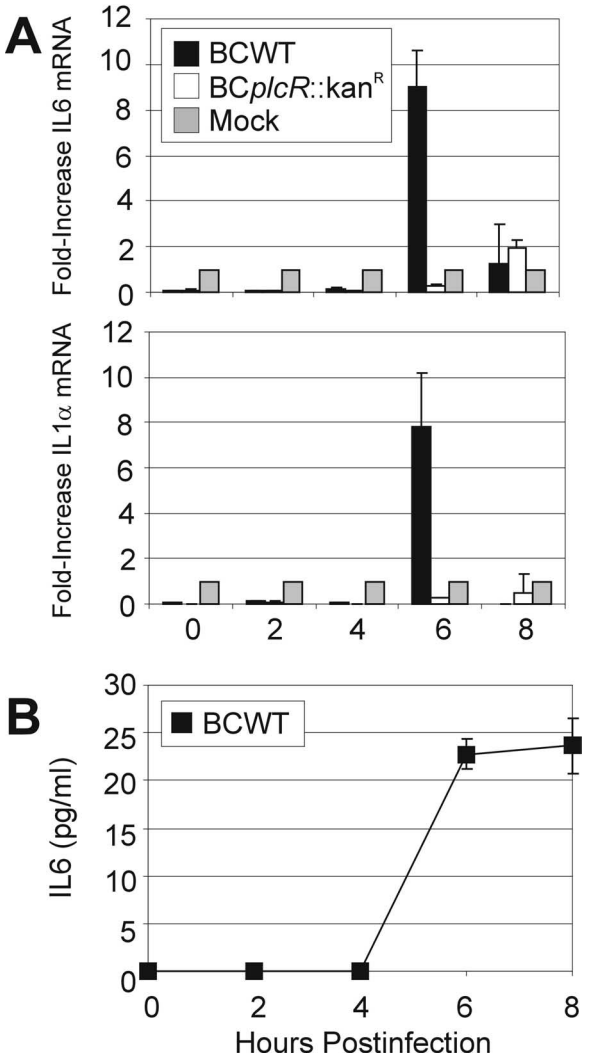

FIG. 9. *B. cereus* infection induces production of IL-6 by RPE cells. RPE cell monolayers were harvested, and total RNA was isolated for production of cDNA with reverse transcriptase. cDNA was amplified by real-time RT-PCR with primers for IL-6, IL-1α, TNF-α, and MIP-1α (A) (mean ± standard deviation; three per group). Only transcripts for IL-6 and IL-1α were detected. RPE cell monolayers were also harvested for analysis of proinflammatory cytokine production by ELISA. IL-6, IL-1α, TNF-α, MIP-1α, IL-1β, and IL-8 were measured by ELISA, but only IL-6 protein was detected (B) (mean ± SEM; six or more per group).

upon infection with any inoculum; however, 10^2 CFU/ml *Bacillus* was selected for subsequent studies because this inoculum produced a course of infection that was optimal for analysis of cellular changes preceding loss of cell viability. Furthermore, 10^2 CFU has been used as the starting inoculum in previous murine and rabbit models of experimental *B. cereus* endophthalmitis (9, 49). We analyzed the growth of both *Bacillus* strains in RPE cell culture medium on RPE cell monolayers and found that both strains grew similarly throughout infection. To ensure that wild-type *Bacillus* produced *plcR*-regulated toxins in RPE cell culture medium, we analyzed the production of hemolysins. During late logarithmic growth, hemolysis was slightly, but not significantly, reduced in RPE cell culture medium (data not shown). These results indicate that the similar phenotypes of the wild-type and *plcR*-deficient *Bacillus* strains grown in each type of medium were not due to a failure of *Bacillus* to produce toxins in RPE cell culture medium.

Bacillus infection caused rapid and complete loss of cell RPE cell viability via necrosis. This is consistent with previous studies demonstrating that *B. cereus* caused loss of cell membrane integrity and viability of other in vitro cells, including retinal Muller cells and corneal keratocytes (10). *B. cereus* has also been shown to induce cytotoxicity in HeLa cells (50) and necrosis of human Caco-2 enterocytes (39). In these Caco-2 enterocytes, the loss of F-actin after infection with *B. cereus* was consistent with epithelial cell necrosis (39). Likewise, unpublished studies in our laboratory indicated that *Bacillus* induced degradation of F-actin and condensation of tubulin around the nucleus. This corroborates our finding that almost all RPE cells undergo necrotic death upon *B. cereus* infection.

Bacillus virulence has been attributed to the production of quorum-sensing-dependent *plcR*-regulated extracellular toxin production. However, this study demonstrated that loss of cell membrane integrity and necrosis occurred independently of *plcR*-regulated toxins. This suggests that a factor or group of factors are produced independently of *plcR* control that may be responsible for this cytotoxic activity. One study suggests that flagellin and InhA2 expression is decreased, but not abolished, in a *plcR* mutant strain of *Bacillus* (28). The ResDE-dependent regulation of enterotoxins may also function partially independently of *plcR* (26). There may also be novel proteases not under the control of *plcR* that are responsible for RPE cell in vitro barrier breakdown (28). Proteases are produced by the *plcR*-deficient *Bacillus* mutant during logarithmic growth in BHI medium (15) and in RPE cell culture medium (data not shown). In both types of medium, the *plcR*-deficient strain has less protease activity than the wild-type *Bacillus* strain. However, future studies will involve analyzing whether proteases, or other toxins, not under *plcR* regulation are responsible for BRB changes during infection.

Taken together, these results demonstrated the deleterious effects of *Bacillus* growth and toxin production on RPE cells. However, to further examine the functional changes that occur in the BRB during infection, it was imperative to develop an in vitro BRB system that structurally and functionally mimicked the in vivo system. Polarization was induced by developing a synthetic matrix for adherence of the basolateral RPE cell surface (33) and optimizing cell culture medium components. Polarization was verified by identifying expression and localization of the Na^+/K^+-ATPase, a primarily apical surface protein (25, 51, 57) that regulates tight junction formation and function during development (65). Tight junction proteins must also be expressed and localized to the cell periphery to maintain barrier function. The Na^+/K^+-ATPase, ZO-1, and occludin were properly localized to the apical surface in our system. Functional tests for polarity also indicated increased TER and decreased permeability to dextran conjugates by 15 days. These factors together indicated that our in vitro BRB mimicked the in vivo system and was sufficient for analysis of barrier changes.

Permeability of polarized RPE cell monolayers occurred as a result of *Bacillus* infection. Permeability of monolayers to dextran conjugates (3, 4, 47) and TER measurements (1, 33)

have been widely used as indicators of RPE cell monolayer integrity and barrier function. Loss of TER has been reported in many in vitro systems to indicate disruption of epithelial tight junction function by pathogens (55). In the present study, TER indicated loss of BRB function by 8 h in response to infection with either strain of *B. cereus*. Again, BRB compromise occurred in the absence of *plcR*-regulated toxins.

The present study suggested that breakdown of RPE cell tight junctions occurred during *Bacillus* infection. Tight junctions form a permeability barrier that defines cell polarity and regulates transepithelial transport. Changes in tight junctions that occur during ocular disease are poorly understood, but these events have been characterized in enterocytes. Some pathogens disrupt tight junctions and alter the intestinal epithelial barrier by secreting toxins. *Pseudomonas* produces an elastase and an alkaline protease that damage tight junctions (59). *Vibrio cholerae* hemagglutinin/protease also perturbs the barrier function of the epithelium by disrupting tight junctions and F-actin (66). Metalloproteases produced by *Bacteroides fragilis* disrupt tight junctions, causing dissociation of occludin and ZO-1 from the tight junction, as well as a reduced TER (55). *Clostridium difficile* exotoxins disaggregate actin, which leads to epithelial cell destruction and loss of tight junctions (45). Proteases have also been shown to break down tight junctions in diseases caused by nonpathogenic organisms (35). The present study demonstrated loss of occludin and ZO-1 upon *B. cereus* infection of RPE cells, suggesting that *Bacillus* produced a toxin, or other enzyme, that contributed to tight junction breakdown by similar proteolytic mechanisms.

It was possible that the loss of tight junctions was not specific but a result of RPE cell death during infection. To determine whether tight junction alterations occurred as a result of cell death or prior to cell death, we analyzed the expression of tight junctions in viable cells alone throughout the infection course. This was done by normalizing tight junction protein expression to that of GAPDH, which is expressed by viable cells. Expression of occludin and ZO-1 decreased in viable cells that had not yet lost membrane integrity, indicating that tight junctions were altered in live cells and not as a result of cell death. It is possible that changes in epithelial tight junctions leads to rapid cell death, resulting in barrier compromise. Although we ultimately see total cell death, this early change in tight junction proteins may be important to the mechanism of barrier disruption.

The immunological response in the eye is quite unique, and RPE cells may have a dynamic role in innate and adaptive ocular immunity. We investigated the possibility that RPE cells produce proinflammatory cytokines and chemokines during infection. However, we only detected IL-6 protein after *B. cereus* infection. RPE cells may produce IL-6 during endophthalmitis to stimulate a local immune response, including recruitment of neutrophils to the barrier in an attempt to clear the infection. However, these data must be confirmed in vivo.

Overall, our results demonstrate the deleterious effect of *Bacillus* growth and toxin production on RPE cells. Permeability of the in vitro BRB occurred independently of *plcR*-regulated toxin production, followed by loss of ZO-1 and occludin, and subsequent tight junction breakdown. Our findings also suggest that the RPE may play a partial role in modulating the immune response by production of IL-6 during infection. Future studies will involve identifying the *B. cereus* factor, or group of factors, that induces BRB barrier permeability during infection. Once putative virulence factors are identified, these will be analyzed in the murine model of endophthalmitis to identify potential mechanisms of barrier breakdown. These virulence factors may prove to be ideal targets for therapeutics that prevent barrier disruption, helping to preserve the vision of patients with *B. cereus* endophthalmitis.

ACKNOWLEDGMENTS

This work was supported by National Institutes of Health grants R01EY12985 (M.C.C.) and P30 EY12190 (NIH CORE Grant to Robert E. Anderson, OUHSC); a Lew R. Wasserman Award from Research to Prevent Blindness, Inc. (M.C.C.); and an unrestricted award from Research to Prevent Blindness, Inc., to the Dean McGee Eye Institute.

We thank Carolanne Roach (Northeastern State University, Tahlequah, OK) and Beryl Ojwang (Oklahoma School for Science and Math) for contributions to this project and Maria Harrington, Jonathan Hunt, Brandt Wiskur, Billy Novosad, Dianca Graham, Dan Carr, and James Chodosh (OUHSC) for technical assistance. We also thank Didier Lereclus (French National Institute for Agricultural Research, Paris, France) for the generous gift of the wild-type and *plcR*-deficient *B. cereus* strains.

We have no conflicts of interest to report.

REFERENCES

1. **Abe, T., E. Sugano, Y. Saigo, and M. Tamai.** 2003. Interleukin-1β and barrier function of retinal pigment epithelial cells (ARPE-19): aberrant expression of junctional complex molecules. Investig. Ophthalmol. Vis. Sci. **44:**4097–4104.
2. **Agaisse, H., M. Gominet, O. A. Okstad, A. B. Kolsto, and D. Lereclus.** 1999. PlcR is a pleiotropic regulator of extracellular virulence factor gene expression in *Bacillus thuringiensis*. Mol. Microbiol. **32:**1043–1053.
3. **Antonetti, D. A., A. J. Barber, S. Khin, E. Lieth, J. M. Tarbell, and T. W. Gardner.** 1998. Vascular permeability in experimental diabetes is associated with reduced endothelial occludin content: vascular endothelial growth factor decreases occludin in retinal endothelial cells. Diabetes **47:**1953–1959.
4. **Bailey, T. A., N. Kanuga, I. A. Romero, J. Greenwood, P. J. Luthert, and M. E. Cheetham.** 2004. Oxidative stress affects the junctional integrity of retinal pigment epithelial cells. Investig. Ophthalmol. Vis. Sci. **45:**675–684.
5. **Barak, A., L. S. Morse, and T. Goldkorn.** 2001. Ceramide: a potential mediator of apoptosis in human retinal pigment epithelial cells. Investig. Ophthalmol. Vis. Sci. **42:**247–254.
6. **Bok, D.** 1982. Autoradiographic studies on the polarity of plasma membrane receptors in retinal pigment epithelial cells, p. 247–256. *In* J. Hollyfield (ed.), The structure of the eye. Elsevier, New York, NY.
7. **Brillard, J., and D. Lereclus.** 2007. Characterization of a small PlcR-regulated gene co-expressed with cereolysin O. BMC Microbiol. **7:**52.
8. **Brillard, J., and D. Lerecluls.** 2004. Comparison of cytotoxin *cytK* promoters from *Bacillus cereus* strain ATCC 14579 and from a *B. cereus* food-poisoning strain. Microbiology **150:**2699–2705.
9. **Callegan, M. C., B. D. Jett, L. E. Hancock, and M. S. Gilmore.** 1999. Role of hemolysin BL in the pathogenesis of extraintestinal *Bacillus cereus* infection assessed in an endophthalmitis model. Infect. Immun. **67:**3357–3366.
10. **Callegan, M. C., D. C. Cochran, S. T. Kane, R. T. Ramadan, J. Chodosh, C. McLean, and D. W. Stroman.** 2006. Virulence factor profiles and antimicrobial susceptibilities of ocular bacillus isolates. Curr. Eye Res. **31:**693–702.
11. **Callegan, M. C., D. Cochran, S. Kane, M. Gilmore, M. Gominet, and D. Lereclus.** 2002. Contribution of membrane-damaging toxins to *Bacillus* endophthalmitis pathogenesis. Infect. Immun. **70:**5381–5389.
12. **Callegan, M. C., M. C. Booth, B. D. Jett, and M. S. Gilmore.** 1999. Pathogenesis of gram-positive bacterial endophthalmitis. Infect. Immun. **67:**3348–3356.
13. **Callegan, M. C., M. Engelbert, D. W. Parke II, B. D. Jett, and M. S. Gilmore.** 2002. Bacterial endophthalmitis: epidemiology, therapeutics, and bacterium-host interactions. Clin. Microbiol. Rev. **15:**111–124.
14. **Callegan, M. C., M. S. Gilmore, M. Gregory, R. T. Ramadan, B. J. Wiskur, A. L. Moyer, J. J. Hunt, and B. D. Novosad.** 2007. Bacterial endophthalmitis: therapeutic challenges and host-pathogen interactions. Prog. Retinal Eye Res. **26:**189–203.
15. **Callegan, M. C., S. T. Kane, C. Cochran, M. S. Gilmore, M. Gominet, and D. Lereclus.** 2003. Relationship of *plcR*-regulated factors to *Bacillus* endophthalmitis virulence. Infect. Immun. **71:**3116–3124.
16. **Callegan, M. C., S. T. Kane, D. C. Cochran, and M. S. Gilmore.** 2002. Molecular mechanisms of *Bacillus* endophthalmitis pathogenesis. DNA Cell Biol. **21:**367–373.
17. **Cellini, M., and A. Baldi.** 1991. Vitreous fluorophotometric recordings in HIV infection. Int. Ophthalmol. **15:**37–40.
18. **Chin, M. S., C. N. Nagineni, L. C. Hooper, B. Detrick, and J. J. Hooks.** 2001. Cyclooxygenase-2 gene expression and regulation in human retinal pigment epithelial cells. Investig. Ophthalmol. Vis. Sci. **42:**2338–2346.

19. **Cousins, S. W., and B. T. Rouse.** 1995. Chemical mediators of ocular disease, p. 50–70. *In* J. S. Pepose, G. N. Holland, K. R. Wilhelmus (ed.), Ocular infection and immunity. C. V. Mosby, St. Louis, MO.
20. **Cousins, S. W., M. M. McCabe, D. Danielpour, and J. W. Streilein.** 1991. Identification of transforming growth factor-β as an immunosuppressive factor in aqueous humor. Investig. Ophthalmol. Vis. Sci. **32:**33–43.
21. **Cowan, C. L., W. M. Madden, G. F. Hatem, and J. C. Merritt.** 1987. Endogenous *Bacillus cereus* panophthalmitis. Ann. Ophthalmol. **19:**65–68.
22. **Cunha-Vaz, J.** 1979. The blood-ocular barriers. Surv. Ophthalmol. **23:**279–296.
23. **Davey, R. T., and W. B. Tauber.** 1987. Posttraumatic endophthalmitis: the emerging role of *Bacillus cereus* infection. Rev. Infect. Dis. **9:**110–123.
24. **Defoe, D. M., A. Ahmad, W. Chen, and B. A. Hughes.** 1994. Membrane polarity of the Na^+-K^+ pump in primary cultures of *Xenopus* retinal pigment epithelium. Exp. Eye Res. **59:**587–596.
25. **Dunn, K. C., A. E. Aotaki-Keen, F. R. Putkey, and L. M. Hjelmeland.** 1996. ARPE-19, a human retinal pigment epithelial cell line with differentiated properties. Exp. Eye Res. **62:**155–169.
26. **Duport, C., A. Zigha, E. Rosenfeld, and P. Schmitt.** 2006. Control of enterotoxin gene expression in *Bacillus cereus* F4430/73 involves the redox-sensitive ResDE signal transduction system. J. Bacteriol. **188:**6640–6651.
27. **Gerry, I., and R. B. Nussenblatt.** 1996. Immunologic basis of uveitis, p. 146–147. *In* J. S. Pepose, G. N. Holland, and K. R. Wilhelmus (ed.), Ocular infection and immunity. C. V. Mosby, St. Louis, MO.
28. **Gohar, M., O. A. Økstad, N. Gilois, V. Sanchis, A. B. Kolsto, and D. Lereclus.** 2002. Two-dimensional electrophoresis analysis of the extracellular proteome of Bacillus cereus reveals the importance of the PlcR regulon. Proteomics **2:**784–791.
29. **Granstein, R., R. Staszewski, T. L. Knisely, E. Zeira, R. Nazareno, M. Latina, and D. M. Albert.** 1990. Aqueous humor contains transforming growth factor-β and a small (<3,500 daltons) inhibitor of thymocyte proliferation. J. Immunol. **144:**3021–3026.
30. **Greenwood, J., R. Howes, and S. Lightman.** 1994. The blood-retinal barrier in experimental autoimmune uveoretinitis. Leukocyte interactions and functional damage. Lab. Investig. **70:**39–52.
31. **Hsueh, Y., E. B. Somers, D. Lereclus, and A. C. Lee Wong.** 2006. Biofilm formation by *Bacillus cereus* is influenced by PlcR, a pleiotropic regulator. Appl. Environ. Microbiol. **72:**5089–5092.
32. **Huber, J. D., C. R. Campos, K. S. Mark, and T. P. Davis.** 2006. Alterations in blood-brain barrier ICAM-1 expression and brain microglial activation following λ-carrageenan induced inflammatory pain. Am. J. Physiol. Heart Circ. Physiol. **290:**H732–H740.
33. **Kim, J. Y., U. S. Sajjan, G. P. Krasan, and J. J. LiPuma.** 2005. Disruption of tight junctions during traversal of the respiratory epithelium by *Burkholderia cenocepacia*. Infect. Immun. **73:**7107–7112.
34. **Kumar, M. V., C. N. Nagineni, M. S. Chin, J. J. Hooks, and B. Detrick.** 2004. Innate immunity in the retina: Toll-like receptor (TLR) signaling in human retinal pigment epithelial cells. J. Neuroimmunol. **153:**7–15.
35. **Lewis, S. A., J. R. Berg, and T. J. Kleine.** 1995. Modulation of epithelial permeability by extracellular macromolecules. Physiol. Rev. **75:**561–589.
36. **Livak, K. J., and T. D. Schmittgen.** 2001. Analysis of relative gene expression data using real-time quantitative PCR and the $2^{-\Delta\Delta C_T}$ method. Methods **25:**402–408.
37. **Magone, M. T., and S. M. Whitcup.** 1999. Mechanisms of intraocular inflammation, p. 90–119. *In* J. W. Streilein, L. Adorini, K. Arai, C. Berek, J. D. Capra, A.-M. Schmitt-Verhulst, and B. H. Waksman (ed.), Immune response and the eye. S. Karger AG, Basel, Switzerland.
38. **Metrikin, D. C., C. A. Wilson, B. A. Berkowitz, M. K. Lam, G. K. Wood, and R. M. Peshock.** 1995. Measurement of blood-retinal barrier breakdown in endotoxin-induced endophthalmitis. Investig. Ophthalmol. Vis. Sci. **36:**1361–1370.
39. **Minnaard, J., M. V. Lievin-Le, M. H. Coconnier, A. L. Servin, and P. F. Perez.** 2004. Disassembly of F-actin cytoskeleton after interaction of *Bacillus cereus* with fully differentiated human intestinal Caco-2 cells. Infect. Immun. **72:**3106–3112.
40. **Miyamoto, K., Y. Ogura, M. Hamada, H. Nishiwaki, N. Hiroshiba, A. Tsujikawa, M. Mandai, K. Suzuma, S. J. Tojo, and Y. Honda.** 1998. In vivo neutralization of P-selectin inhibits leukocyte-endothelial interaction in retinal microcirculation during ocular inflammation. Microvasc. Res. **55:**230–240.
41. **Momma, Y., C. N. Nagineni, M. S. Chin, K. Srinivasan, B. Detrick, and J. J. Hooks.** 2003. Differential expression of chemokines by human retinal pigment epithelial cells infected with cytomegalovirus. Investig. Ophthalmol. Vis. Sci. **44:**2026–2033.
42. **O'Day, D. M., R. S. Smith, C. R. Gregg, P. C. B. Turnbull, W. S. Head, J. A. Ives, and P. C. Ho.** 1981. The problem of *Bacillus* species infection with special emphasis on the virulence of *Bacillus cereus*. Ophthalmology **88:**833–838.
43. **Okami, T., A. Yamamoto, K. Omori, T. Takada, M. Uyama, and Y. Tashiro.** 1990. Immunocytochemical localization of Na^+,K^+-ATPase in rat retinal pigment epithelial cells. J. Histochem. Cytochem. **38:**1267–1275.
44. **Okstad, O. A., M. Gominet, B. Purnelle, M. Rose, D. Lereclus, and A. Kolsto.** 1999. Sequence analysis of three *Bacillus cereus* loci carrying PlcR-regulated genes encoding degradative enzymes and enterotoxin. Microbiology **145:** 3129–3138.
45. **Pepose, J. S., G. N. Holland, M. S. Nestor, A. J. Cochran, and R. Y. Foos.** 1985. Acquired immune deficiency syndrome: pathogenic mechanisms of ocular disease. Ophthalmology **92:**472–484.
46. **Percopo, C. M., J. J. Hooks, T. Shinohara, R. Caspi, and B. Detrick.** 1990. Cytokine-mediated activation of a neuronal retinal resident cell provides antigen presentation. J. Immunol. **145:**4101–4107.
47. **Pitkanen, L., V. Ranta, H. Moilanen, and A. Urtti.** 2005. Permeability of retinal pigment epithelium: effects of permeant molecular weight and lipophilicity. Investig. Ophthalmol. Vis. Sci. **46:**641–646.
48. **Planck, S. R., X. N. Huang, J. E. Robertson, and J. T. Rosenbaum.** 1993. Retinal pigment epithelial cells produce interleukin-1β and granulocyte-macrophage colony-stimulating factor in response to interleukin-1α. Curr. Eye Res. **12:**205–212.
49. **Ramadan, R. T., R. Ramirez, B. D. Novosad, and M. C. Callegan.** 2006. Acute inflammation and loss of retinal architecture and function during experimental *Bacillus* endophthalmitis. Curr. Eye Res. **31:**1–11.
50. **Ramarao, N., and D. Lereclus.** 2006. Adhesion and cytotoxicity of Bacillus cereus and Bacillus thuringiensis to epithelial cells are FlhA and PlcR dependent, respectively. Microbes Infect. **8:**1483–1491.
51. **Rizzolo, L. J.** 1999. Polarization of the Na^+,K^+-ATPase in epithelia derived from the neuroepithelium. Int. Rev. Cytol. **185:**195–235.
52. **Rizzolo, L. J., Y. Luo, Y. Zhuo, and M. Fukuhara.** 2006. Effects of culture conditions on heterogeneity and the apical junctional complex of the ARPE-19 cell line. Investig. Ophthalmol. Vis. Sci. **47:**3644–3655.
53. **Salamitou, S., F. Ramisse, M. Brehelin, D. Bourguet, N. Gilois, M. Gominet, E. Hernandez, and D. Lereclus.** 2000. The *plcR* regulon is involved in the opportunistic properties of *Bacillus thuringiensis* and *Bacillus cereus* in mice and insects. Microbiology **146:**2825–2832.
54. **Scott, I. U., H. W. Flynn, W. Feuer, S. C. Pflugfelder, E. C. Alfonso, R. K. Forster, and D. Miller.** 1996. Endophthalmitis associated with microbial keratitis. Ophthalmology **103:**1864–1870.
55. **Sears, C.** 2000. Molecular physiology and pathophysiololgy of tight junctions. V. Assault of the tight junction by enteric pathogens. Am. J. Physiol. Gastrointest. Liver Physiol. **279:**G1129–G1134.
56. **Shamsuddin, D., C. U. Tuazon, C. Levy, and J. Curtin.** 1982. *Bacillus cereus* panophthalmitis: source of the organism. Rev. Infect. Dis. **4:**97–103.
57. **Steuer, H., A. Jaworski, D. Stoll, and B. Schlosshauer.** 2004. In vitro model of the outer blood-retina barrier. Brain Res. Protocols **13:**26–36.
58. **Streilein, J. W.** 1999. Regional immunity and ocular immune privilege, p. 11–38. *In* J. W. Streilein, L. Adorini, K. Arai, C. Berek, J. D. Capra, A.-M. Schmitt-Verhulst, and B. H. Waksman (ed.), Immune response and the eye. S. Karger AG, Basel, Switzerland.
59. **Suter, S.** 1994. The role of bacterial protease in the pathogenesis of cystic fibrosis. Am. J. Respir. Crit. Care Med. **150:S**118–S122.
60. **Taylor, A. W.** 1999. Ocular immunosuppressive microenvironment, p. 72–89. *In* J. W. Streilein, L. Adorini, K. Arai, C. Berek, J. D. Capra, A.-M. Schmitt-Verhulst, and B. H. Waksman (ed.), Immune response and the eye. S. Karger AG, Basel, Switzerland.
61. **Taylor, A. W., D. G. Yee, and J. W. Streilein.** 1998. Suppression of nitric oxide generated by inflammatory macrophages by calcitonin gene-related peptide in aqueous humor. Investig. Ophthalmol. Vis. Sci. **39:**1372–1378.
62. **Taylor, A. W., J. W. Streilein, and S. W. Cousins.** 1992. Identification of alpha-melanocyte stimulating hormone as a potential immunosuppressive factor in aqueous humor. Curr. Eye Res. **11:**1199–1206.
63. **Taylor, A. W., J. W. Streilein, and S. W. Cousins.** 1994. Immunoreactive vasoactive intestinal peptide contributes to the immunosuppressive activity of normal aqueous humor. J. Immunol. **153:**1080–1086.
64. **Vinores, S. A., A. Amin, N. L. Derevjanik, W. R. Green, and P. A. Campochiaro.** 1994. Immunohistochemical localization of blood-retinal barrier breakdown sites associated with post-surgical macular edema. Histochem. J. **26:**655–665.
65. **Violette, M. I., P. Madan, and A. J. Watson.** 2006. Na^+/K^+-ATPase regulates tight junction formation and function during mouse preimplantation development. Dev. Biol. **289:**406–419.
66. **Wu, Z., P. Nybom, and K. E. Magnusson.** 2000. Distinct effects of Vibrio cholerae haemagglutinin/protease on the structure and localization of the tight junction-associated proteins occluding and ZO-1. Cell. Microbiol. **2:**11–17.
67. **Xu, H., J. V. Forrester, J. Liversidge, and I. J. Crane.** 2003. Leukocyte trafficking in experimental autoimmune uveitis: breakdown of blood-retinal barrier and upregulation of cellular adhesion molecules. Investig. Ophthalmol. Vis. Sci. **44:**226–234.
68. **Xu, H., R. Dawson, I. Crane, and J. Liversidge.** 2005. Leukocyte diapedesis in vivo induces transient loss of tight junction protein at the blood-retinal barrier. Investig. Ophthalmol. Vis. Sci. **46:**2487–2494.

Editor: B. A. McCormick